Characterization of Thermal Arc Generator RB3 Flows by Laser Absorption Spectroscopy and Pitot Probe

Makoto MATSUI*, Hiroki TAKAYANAGI*, Andreas KNAPP**, Georg HERDRICH**, Kimiya KOMURASAKI***, Yoshihiro ARAKAWA* and Monika AUWETER-KURTZ****

*Department of Aeronautics and Astronautics, University of Tokyo,

** Institut für Raumfahrtsysteme, University of Stuttgart,

***Department of Advanced Energy, University of Tokyo,

****University of Hamburg

Abstract

The thermal arc generator RB3 flows were characterized by laser absorption spectroscopy and Pitot probe measurement. Firstly, translational temperature and flow velocity distributions in an argon flow were deduced from measured absorption profile of ArI 772.42 nm. The averaged specific enthalpy and plasma power for TPS test region was estimated as 3.72±0.48 MJ/kg, 1.77±0.68 kW, respectively. Next, an air flow was diagnosed using OI 777.19 nm line. The specific enthalpy on the axis was estimated from the deduced temperature, Mach number and thermo-chemical equilibrium assumption in the plenum. As a result, the specific enthalpy, the degree of dissociation in oxygen and nitrogen were estimated as 11.1±1.8 MJ/kg, 88.5 % and 3.8 %, respectively.

Keywords: High enthalpy flow, Thermal arc generator, Atomic oxygen, Laser absorption spectroscopy

1. Introduction

In developing thermal protection systems (TPS) for reentry vehicles, arc-heaters are widely used to simulate such high enthalpy flows because it has a simple and rugged structure, long operational time and relatively ease of maintenance [1, 2].

In conventional passive TPS tests, atomic oxygen has been found to play important roles through heat-flux enhancement by catalytic effects and active–passive oxidation of TPS surfaces [3,4]. However, their exact flow conditions are mostly unknown because they are usually in strong thermo-chemical non-equilibrium. Although nonintrusive spectroscopic methods such as emission spectroscopy and laser induced florescence spectroscopy have been actively applied to the characterization of such high enthalpy flows, it is still difficult to measure the chemical compositions by these spectroscopic methods [5].

Recently, electromagnetic flow control has got an attention as active TPS [6, 7]. This system utilizes the electromagnetic effect from on-board magnetic source to reduce aerodynamic heating and increase aerodynamic drag. Currently as a basic research, influence of a magnetic probe on a weakly ionized argon flow generated by an arc-heater has been experimentally and numerically studied [8-10]. Then, flow conditions are essential for such research.

In this study, laser absorption spectroscopy (LAS) and Pitot probe were applied to the thermal arc generator RB3 to characterize argon and air flows. The specific enthalpy and degree of dissociation in oxygen and nitrogen were estimated.

2. Experimental Procedure

2.1 Thermal arc generator RB3

The thermal arc generator RB3 was developed at the Institut für Raumfahrtsysteme (IRS) at the University of Stuttgart [11]. **Figure 1** shows a schematic of the RB3. The RB3 has a bi-throat design. The nitrogen is supplied from the base of the cathode made of 2 % thoriated tungsten. On the other hand, the oxygen is injected at the downstream of the anode towards the nozzle throat to prevent the cathode from oxidation. In order to reduce anode erosion, an axial magnetic field is applied by a coil to move an arc spot rapidly around.

Two kinds of working gases were used; argon and air. Here, the air was simulated with nitrogen and oxygen. The operation conditions are listed in **Table 1**.

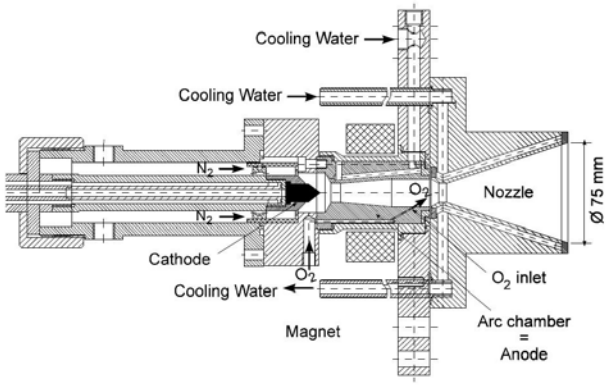

Fig.1 A schematic of thermal arc generator RB3.

Table 1 Operation conditions.

	Argon	Air
Working gas	Ar 5 g/s	N_2: 2.4 g/s O_2: 0.6 g/s
Input power	16 kW (650 A)	65 kW (800 A)
Plenum pressure	19.4 kPa	23.6 kPa
Ambient pressure	255 Pa	258 Pa

2.2 Laser absorption spectroscopy

In our experimental condition, Doppler broadening is several gigahertzes, which is two orders of magnitude greater than all other broadenings, including natural, pressure and Stark broadenings [12-13]. The absorption profile $k(\nu)$ at the laser frequency ν is approximated as a Gaussian profile, expressed as,

$$k(\nu) = \frac{2K}{\Delta\nu_D}\sqrt{\frac{\ln 2}{\pi}}\exp\left[-\ln 2\left\{\frac{2(\nu-\nu_0-\nu_{shift})}{\Delta\nu_D}\right\}^2\right]. \quad (1)$$

Here, ν_0 is the center absorption frequency and K is the integrated absorption coefficient.

$\Delta\nu_D$ is the full width at half maximum of the profile and is related to the translational temperature T, expressed as

$$\Delta\nu_D = 2\nu_0\sqrt{\frac{2k_BT}{mc^2}\ln 2}, \quad (2)$$

where m, c and k_B represent the mass of absorbers, velocity of light, and the Boltzmann constant, respectively.

ν_{shift} is the shift of the center absorption frequency by Doppler shift and is related to the flow velocity u, expressed as,

$$\nu_{shift} = \frac{u\cdot\nu_0}{c}\cos\theta, \quad (3)$$

where θ is the incident laser beam angle to the flow.

Figure 2 shows a schematic of the LAS measurement system. A tunable diode-laser with an external cavity (Velocity Model 6300, New Focus, Inc.) was used as the laser oscillator. Its line width is less than 300 kHz. The laser frequency was scanned over the absorption line shape. The modulation frequency and width were 1 Hz and 30 GHz, respectively. The laser intensity was sufficiently small to avoid the influence of absorption saturation [14]. An optical isolator was used to prevent the reflected laser beam from returning into the external cavity. An etalon was used as a wave-meter. Its free spectral range was 0.75 GHz.

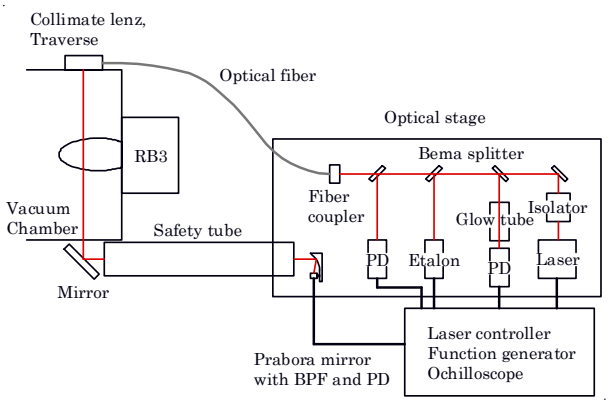

Fig.2 LAS measurement system.

The probe beam was guided to the chamber window through an optical fiber. The fiber output was mounted on a one-dimensional traverse stage to scan the flow in the radial direction. The probe beam diameter was 2 mm at the chamber center. To reduce plasma emission, transmitted laser intensity was measured at 3 m away from the plume using a photo detector (DET110/M, Thorlabs, Inc.) with a 2-mm pinhole and a band-pass filter whose full width at half maximum was 10 nm. A parabola mirror allowed scanning of the plume without synchronizing the detector position with the probe beam position. Signals were recorded using a digital oscilloscope (NR-2000, Keyence Co.) with 14-bit resolution at the sampling rate of 20 kHz. The target lines were those of argon at 772.42 nm and atomic oxygen at 777.19 nm.

2.3 Pitot probe

The Pitot probe developed at IRS was used to measure the Mach number. **Figure 3** shows a schematic of the Pitot probe. This probe is geometrically similar to the material support system for TPS tests. This is so-called European standard geometry; the outer diameter of 50 mm and corresponding on material sample diameter of 26.5 mm [11].

The ratio of the Pitot pressure p_{Pitot} to the ambient pressure p_{amb} is related to the Mach number M by Rayleigh supersonic Pitot formula, expressed as

$$\frac{p_{Pitot}}{p_{amb}} = \left[\frac{(\gamma+1)M^2}{2}\right]^{\frac{\gamma}{\gamma-1}}\left[\frac{\gamma+1}{2\gamma M^2-(\gamma-1)}\right]^{\frac{1}{\gamma-1}}, \quad (4)$$

where γ is the specific heat ratio. **Figure 4** shows calculated Mach number as a function of the pressure ratio for the various specific heat ratios.

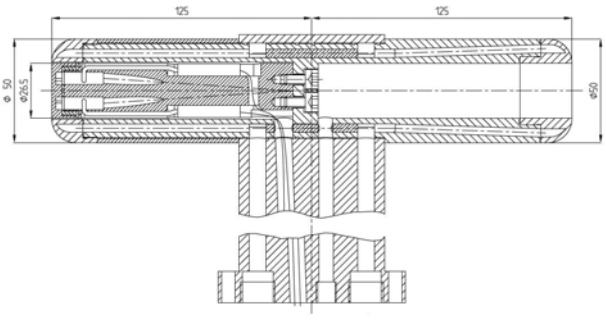

Fig. 3 A schematic of Pitot probe.

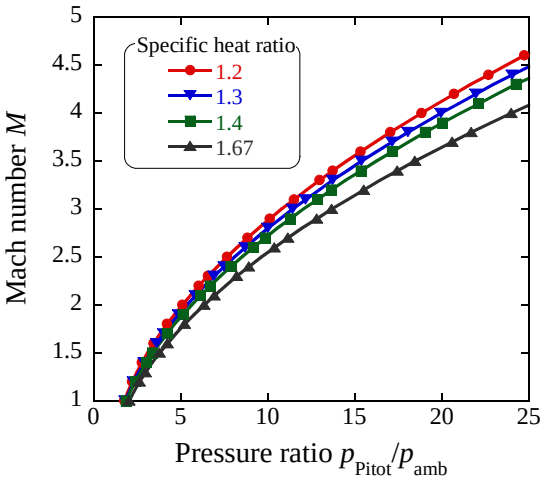

Fig. 4 Mach number as a function of the pressure ratio for the various specific heat ratios.

3. Results and Discussion

3.1 Argon flow diagnostics

Figure 5 shows a photo of the argon plume. The measured plane was 100 mm away from the nozzle exit. The incident laser beam angle to the flow was 85.2 degree. The eight absorption signals were measured every 3 mm in the range of $0<x<42$ mm. Here, x is the distance between the flow axis and the laser path. Typical absorption signals in the flow and the glow tube and etalon signal are shown in **Fig.6**. Because the measured signals are composed of path-integrated absorption coefficient, Abel inversion was applied to obtain the local absorption coefficient. When axisymmetric distributions of flow properties are assumed, the absorption coefficient is obtained by the Abel inversion as,

$$k(\nu)=\frac{1}{\pi}\int_r^R \frac{d\left\{\ln\left[(I/I_0(x,\nu_0))\right]\right\}/dx}{\sqrt{x^2-r^2}}dx, \qquad (5)$$

Here, r is the radial coordinate and the R is the plume radius. The absorption coefficients are dependent on the frequency. Then the Abel inversion should be conducted frequency by frequency. Here, after

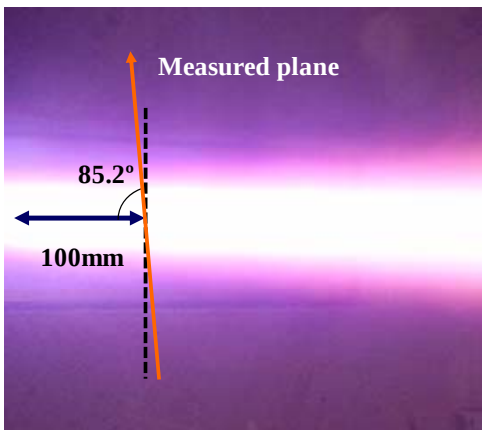

Fig. 5 Photo of the argon plume.

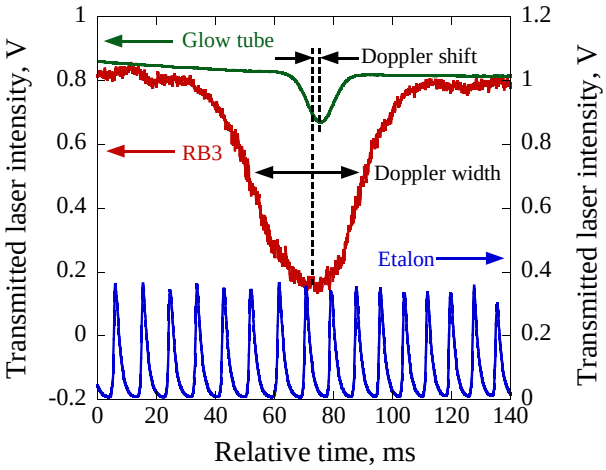

Fig. 6 Typical transmitted laser and etalon signals.

curve fitting to the path-integrated absorption profiles, the absorbance is extracted every 0.05 GHz from the fitted curves, and then the absorption profile is calculated by numerical integral [15].

Figure 7 shows deduced temperature and the velocity distributions from measured broadening width of the profile and the shift. On the axis, both distributions have peak values of 4414 K and 3190 m/s, respectively.

In this experimental condition, the degree of ionization would be so small that the chemical potential is neglected and the specific heat ratio at the constant pressure C_p is assumed almost constant for the variation of temperature. Thereby, the specific enthalpy h is expressed as,

$$h(r)=C_pT(r)+\frac{1}{2}u(r)^2. \qquad (6)$$

The plasma power P is defined as,

$$P(r)=\int_0^r 2\pi r\rho(r)u(r)h(r)dr, \qquad (7)$$

where ρ is the density expressed as $\rho=p_{amb}/k_BT$.

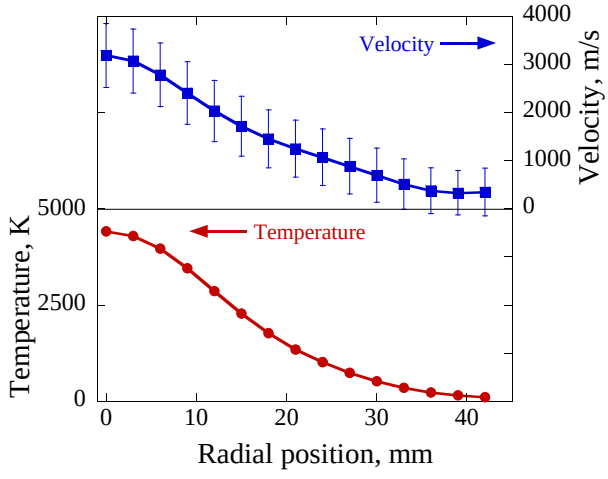

Fig. 7 Temperature and velocity distributions.

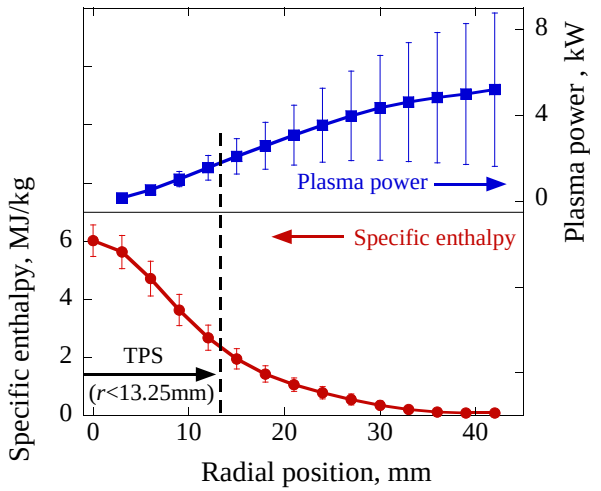

Fig. 8 Specific enthalpy and plasma power distributions.

Figure 8 shows distributions of the specific enthalpy and the plasma power. The averaged specific enthalpy and plasma power for the TPS test region (r<13.25 nm) were 3.72 ± 0.48 MJ/kg and 1.77 ± 0.68 kW, respectively. This value corresponds to 10.9 % of the input power.

3.2 Air flow diagnostics

Figure 9 shows measured absorbance on the axis at 100 mm from the nozzle exit. In the air flow, the absorption signal was too small to be detected off-axis. Then, the profile on the axis was analyzed without Abel inversion. The deduced temperature from the line broadening was 3237±303 K. Here, the error was the standard deviation of eight profiles.

Since there was not stationary atomic oxygen source, the velocity was estimated from the measured Mach number by the Pitot probe using.

$$u = M\sqrt{\gamma RT}\ . \qquad (8)$$

where, R is the gas constant.

Figure 10 shows measured Pitot pressure distributions and deduced Mach number distribution using Eq. (4). The Mach number on the axis was estimated as 1.94.

The specific enthalpy and degree of dissociation in oxygen and nitrogen were estimated as follows. Assuming an isentropic expansion and chemically frozen flow between the plenum and the plume, the total specific enthalpy is estimated as,

$$\begin{aligned} h &= \int_0^{T_0} C_p dT' + h_{\text{chem}} \qquad \text{(Plenum)} \\ &= \int_0^{T} C_p dT' + h_{\text{chem}} + \frac{1}{2}u^2 \qquad \text{(Plume)} \end{aligned} \quad . \qquad (9)$$

Here, T_0 is the total temperature and h_{chem} is the chemical potential. Since the total pressure measured in the plenum was as high as 23.6 kPa, the chemical composition in the discharge part was calculated by assuming thermo-chemical equilibrium. In the calculation, the following 11 chemical species were considered: N_2, O_2, N, O, NO, N_2^+, O_2^+, N^+, O^+, NO^+, and e^-. Their equilibrium constants were obtained from Ref. 16. In addition, the specific heat at a constant pressure, the gas constant and the specific heat ratio were computed as the sum of the contributions of all species. **Figure 11** shows the calculated mole fraction and specific enthalpy as a function of the total temperature. The deduced temperature by Eq. (9) was 5350 K.

As a result, the estimated specific enthalpy, the degree of dissociation in oxygen and nitrogen were 11.1±1.8 MJ/kg, 88.5% and 3.8 %, respectively.

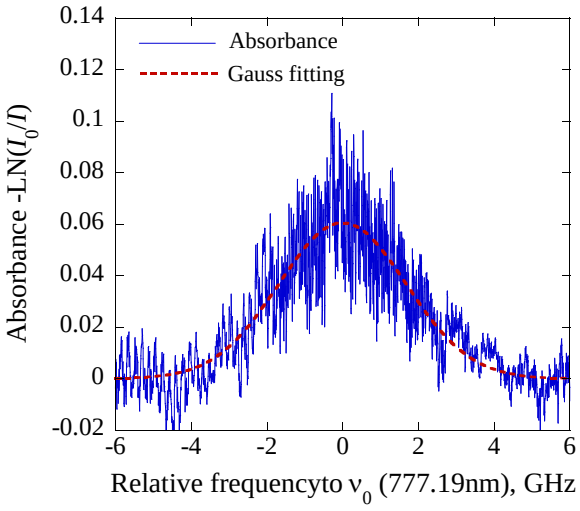

Fig. 9 Measured absorbance and a Guass fit.

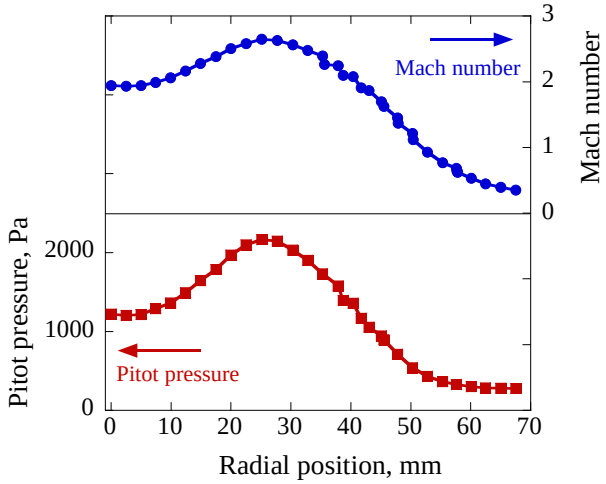

Fig. 10 Pitot pressure and deduced Mach number distributions.

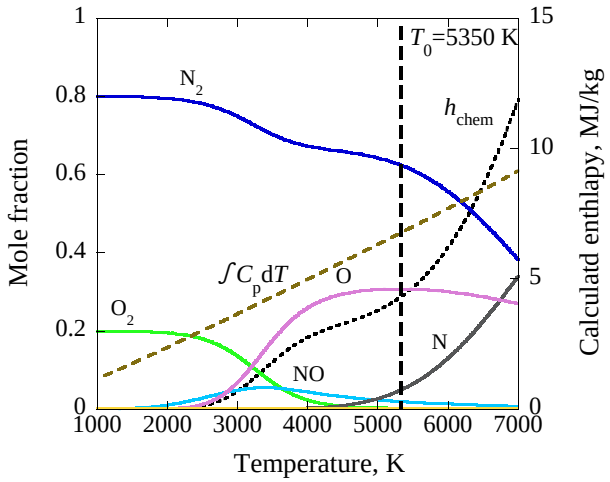

Fig. 11 Calculated enthalpy and mole fractions by thermo-chemical equilibrium assumptions, p_0=23.6 kPa.

4. Conclusions

The thermal arc generator RB3 flows were characterized by laser absorption spectroscopy and Pitot probe as follows.

(1) In the argon flow, the translational temperature and the flow velocity distributions measured by LAS using ArI 772.42 nm line have peak values of 4414 K and 3190 m/s on the axis.

(2) The averaged specific enthalpy and the plasma power for the TPS test region were estimated as 3.72±0.48 MJ/kg and 1.77±0.68 kW, respectively. This value corresponds to 10.9 % of the input power.

(3) In the air flow, the absorption signal of OI 777.19 nm line was detected only on the axis resulting in the deduced temperature of 3237±303 K.

(4) The Mach number measured by Pitot probe was 1.94 on the axis.

(5) The specific enthalpy, degree of dissociation in oxygen and nitrogen on the axis were estimated as 11.1±1.8 MJ/kg, 88.5 % and 3.8 %, respectively.

Acknowledgment

This work was partially supported by Research Fellowships of the Japan Society for the Promotion of Science for Young Scientists, 18-09885.

References

1) M. Auweter-Kurtz, H. Kurtz, and S. Laure, “Plasma Generators for Reentry Simulation,” *J. Propul. Power*, **12**-6 (1996), 1053–1061.

2) M. A. Birkan, “Arcjets and Arc Heaters: An Overview of Research Status and Needs,” *J Propul. Power*, **12**-6 (1996), 1011–1017.

3) N. G. Bykova, S. A. Vasil’evskii, A. N. Gordeev, A. F. Kolesnikov, I. S. Pershin, and M. I. Yakushin, “Determination of the Effective Probabilities of Catalytic Reactions on the Surfaces on Heat Shield Materials in Dissociated Carbon Dioxide Flows,” *Fluid Dyn.*, **32**-6 (1997), 876–886.

4) M. Balat, G. Flamant, G. Male, and G. Pichelin, “Active to Passive Transition in the Oxidation of Silicon Carbide at High Temperature and Low Pressure in Molecular and Atomic Oxygen,” *J Mater. Sci.*, **27**-3 (1992), 697–703.

5) M. Matsui, H. Takayanagi, Y. Oda, K. Komurasaki, and Y. Arakawa, “Estimation of Atomic Oxygen Concentration by Semi-empirical Collisional Radiative Model in High Enthalpy Flow,” *AIAA Paper* 04-2473 (2004).

6) E. L. Resler, and W. R. Sears, “The Prospects of Magnetoaerodynamics,” *J. Aero. Sci.*, **25** (1958), 235–245.

7) W. B. Ericson, and A. Maciulaitis, “Investigation of Magnetohydrodynamic Flight Control,” *J Spacecraft and Rockets*, **1**-3 (1964), 283–289.

8) A. Knapp, M. Fertig, D. Haag, and G. Herdrich, and M. Auweter-Kurtz, “Investigation of the Interaction between a Magnetic Probe Body and Argon Plasma”, *AIAA Paper* 07-4133 (2007).

9) A. Knapp, D. Haag, M. Fertig, G. Herdrich, M. Auweter-Kurtz, “Analysis of the Influence of Permanent Magnets on Argon Plasma Flow”, *App. Plasma Sci.* **15**-2 (2008),149-155.

10) H. Katsurayama, D. Konigorski, and T. Abe, “Numerical Simulation of Electromagnetic Flow Control in an Arcjet Plume”, *AIAA Paper* 08-1392 (2008).

11) Auweter-Kurtz, M., “Overview of IRS Plasma Wind Tunnel Facilities,” Measurement Techniques for High Enthalpy and Plasma Flows, NATO Research and Technology Organization proceedings RTO-EN-8, Neuilly-Sur-Seine Cedex, France, 2A-1-1A-20 (2000).

12) M. Matsui, K. Komurasaki, Y. Arakawa, A. Knapp, G. Herdrich, M. Auweter-Kurtz, M., “Enthalpy Measurement of Inductively Heated Air Flow,” *J. Spacecraft Rockets*, 45, 155-157 (2008).

13) M. Matsui, T. Ikemoto, H. Takayanagi, K. Komurasaki, and Y. Arakawa, “Generation of Highly Dissociated Oxygen Flows Using a Constrictor-Type Arc-Heater,” *J Thermophys. Heat Tr.*, 21-1 (2007), 247–249.

14) Matsui, M., Ogawa, S., Komurasaki, K., and Arakawa, Y., “Influence of Laser Intensity on Absorption Line Broadening in Laser Absorption Spectroscopy,” *J. Appl. Phys*, 100, 063102 (2006).

15) C. J. Dasch, "One-dimensional tomography: a comparison of Abel, onion-peeling, and filtered back projection methods," *Appl. Opt.* **31** (1992) 1146-1152.

16) Guputa, R. N., Yos, J. M., Thompson, R. A., and Lee, K. P., “A Review of Reaction Rates and Thermodynamic and Transport Properties for an 11-Species Air Model for Chemical and Thermal Nonequilibrium Calculations to 30000K,” NASA Reference Publication 1232 (1990).